Published in final edited form as:
Bioconjug Chem. 2012 June 20; 23(6): 1341–1348. doi:10.1021/bc300191z.

Gallium-67-Labeled Lactam Bridge-Cyclized Alpha-MSH Peptides with Enhanced Melanoma Uptake and Reduced Renal Uptake

Haixun Guo[†], **Fabio Gallazzi**[§], and **Yubin Miao**[†,⊥,φ,*]

[†]College of Pharmacy, University of New Mexico, Albuquerque, NM 87131, USA

[⊥]Cancer Research and Treatment Center, University of New Mexico, Albuquerque, NM 87131, USA

[φ]Department of Dermatology, University of New Mexico, Albuquerque, NM 87131, USA

[§]Department of Biochemistry, University of Missouri, Columbia, MO 65211, USA

Abstract

The purpose of this study was to examine the melanoma targeting and pharmacokinetic properties of ^{67}Ga-DOTA-GGNle-CycMSH$_{hex}$ {^{67}Ga-1,4,7,10-tetraazacyclononane-1,4,7,10-tetraacetic acid-Gly-Gly-Nle-c[Asp-His-$_D$Phe-Arg-Trp-Lys]-CONH$_2$} and ^{67}Ga-NOTA-GGNle-CycMSH$_{hex}$ {^{67}Ga-1,4,7-triazacyclononane-1,4,7-triacetic acid-Gly-Gly-Nle-c[Asp-His-$_D$Phe-Arg-Trp-Lys]-CONH$_2$} and compare with ^{67}Ga-DOTA-GlyGlu-CycMSH {^{67}Ga-DOTA-Gly-Glu-c[Lys-Nle-Glu-His-$_D$Phe-Arg-Trp-Gly-Arg-Pro-Val-Asp]} we previously reported. DOTA-GGNle-CycMSH$_{hex}$ and NOTA-GGNle-CycMSH$_{hex}$ were synthesized using fluorenylmethyloxy carbonyl (Fmoc) chemistry. The melanocortin-1 (MC1) receptor binding affinity of NOTA-GGNle-CycMSH$_{hex}$ was determined in B16/F1 melanoma cells and compared with DOTA-GGNle-CycMSH$_{hex}$. The melanoma targeting and pharmacokinetic properties of ^{67}Ga-NOTA-GGNle-CycMSH$_{hex}$ and ^{67}Ga-DOTA-GGNle-CycMSH$_{hex}$ were determined in B16/F1 melanoma-bearing C57 mice. NOTA-GGNle-CycMSH$_{hex}$ and DOTA-GGNle-CycMSH$_{hex}$ displayed comparable MC1 receptor binding affinities (1.6 vs. 2.1 nM) in B16/F1 melanoma cells. Both ^{67}Ga-NOTA-GGNle-CycMSH$_{hex}$ and ^{67}Ga-DOTA-GGNle-CycMSH$_{hex}$ exhibited dramatically enhanced melanoma uptake and reduced renal uptake than ^{67}Ga-DOTA-GlyGlu-CycMSH in B16/F1 melanoma-bearing C57 mice. Furthermore, ^{67}Ga-NOTA-GGNle-CycMSH$_{hex}$exhibited more favorable radiolabeling conditions (> 85% radiolabeling yields started at 37°C), as well as higher tumor/kidney uptake ratios than ^{67}Ga-DOTA-GGNle-CycMSH$_{hex}$ at 0.5, 2 and 24 h post-injection. High melanoma uptake coupled with low renal uptake highlighted the potential of ^{67}Ga-NOTA-GGNle-CycMSH$_{hex}$for melanoma imaging and therapy.

Keywords

Alpha-melanocyte stimulating hormone; ^{67}Ga-labeled; lactam bridge-cyclized peptide; melanoma targeting

Corresponding Author: Yubin Miao, 2502 Marble NE, MSC09 5360, College of Pharmacy, University of New Mexico, Albuquerque, NM 87131, USA. Phone: (505) 925-4437; Fax: (505) 272-6749; ymiao@salud.unm.edu.

INTRODUCTION

It is highly desirable to develop novel melanoma-specific diagnostic and therapeutic agents[1–18] for melanoma since no curative treatment is available for patients with metastatic melanoma. Over the past several years, we and others have been interested in developing lactam bridge-cyclized alpha-melanocyte stimulating hormone (α-MSH) peptide radiopharmaceuticals targeting melanocortin-1 (MC1) receptors for melanoma imaging.[19–26] Specifically, we have developed two generations of ^{111}In-labeled novel lactam bridge-cyclized α-MSH peptides for melanoma targeting.[19–24] The first-generation peptides were designed based on the construct of CycMSH peptide {c[Lys-Nle-Glu-His-$_D$Phe-Arg-Trp-Gly-Arg-Pro-Val-Asp}], which was a 12-amino acid-peptide cyclized by a Lys-Asp lactam bridge. The second-generation peptides built upon the backbone of $CycMSH_{hex}$ peptide {c[Asp-His-$_D$Phe-Arg-Trp-Lys]-$CONH_2$}, which was a 6-amino acid-peptide cyclized by an Asp-Lys lactam bridge. The structural modifications from the first-generation peptides to the second-generation peptides enhanced melanoma uptake and reduced renal uptake of ^{111}In-labeled $CycMSH_{hex}$ peptides.[19–24] For instance, ^{111}In-DOTA-Nle-$CycMSH_{hex}$ displayed higher melanoma uptake (19.39 ± 1.65 % ID/g at 2 h post-injection) and lower renal uptake (9.52 ± 0.44 % ID/g at 2 h post-injection) than ^{111}In-DOTA-GlyGlu-CycMSH in B16/F1 melanoma-bearing C57 mice.[19,23]

In 2009, we reported ^{67}Ga-DOTA-GlyGlu-CycMSH[22] as a potential melanoma imaging agent taking advantage of the diagnostic properties of ^{67}Ga ($T_{1/2}$= 78.3 h, 93, 185 and 300 keV γ-emissions). Both flank primary B16/F1 melanoma and B16/F10 pulmonary melanoma metastases were clearly visualized by SPECT/CT using ^{67}Ga-DOTA-GlyGlu-CycMSH as an imaging probe 2 h post-injection.[22] However, despite the substantial tumor uptake (12.93 ± 1.63 %ID/g at 2 h post-injection), ^{67}Ga-DOTA-GlyGlu-CycMSH also exhibited relatively high renal uptake (27.55 ± 7.87 %ID/g at 2 h post-injection) in B16/F1 melanoma-bearing C57 mice.[22] It is important to note that ^{67}Ga is also a potential therapeutic radionuclide because of its emissions of Auger and conversion electrons.[27] Hence, we managed to reduce the renal uptake of ^{67}Ga-DOTA-GlyGlu-CycMSH via *L*-lysine co-injection to facilitate its potential therapeutic application. *L*-lysine co-injection successfully decreased the renal uptake of ^{67}Ga-DOTA-GlyGlu-CycMSH by 69.8% without affecting the melanoma uptake at 2 h post-injection.[22]

Structural modification on peptide sequence is another way to reduce the renal uptake of radiolabeled α-MSH peptides.[22–24] Recently, we found that ^{111}In-DOTA-GGNle-$CycMSH_{hex}$ displayed higher B16/F1 melanoma uptake (19.05 ± 5.04 % ID/g at 2 h post-injection) and reduced renal uptake (6.84 ± 0.92 % ID/g at 2 h post-injection) compared to ^{111}In-DOTA-GlyGlu-CycMSH.[22–24] Therefore, we hypothesized that ^{67}Ga-DOTA-GGNle-$CycMSH_{hex}$ would exhibit enhanced melanoma uptake and reduced renal uptake than ^{67}Ga-DOTA-GlyGlu-CycMSH. To examine our hypothesis, we determined the biodistribution of ^{67}Ga-DOTA-GGNle-$CycMSH_{hex}$ in B16/F1 melanoma-bearing C57 mice in this study. Despite the fact that DOTA can form stable complexes with a variety of radionuclides including ^{67}Ga, NOTA can also form stable complex with ^{67}Ga at lower reaction temperature.[28–29] Thus, we also determined the melanoma targeting and pharmacokinetic properties of ^{67}Ga-NOTA-GGNle-$CycMSH_{hex}$in B16/F1 melanoma-bearing C57 mice in this study.

EXPERIMENTAL PROCEDURES

Chemicals and Reagents

Amino acid and resin were purchased from Advanced ChemTech Inc. (Louisville, KY) and Novabiochem (San Diego, CA). NO2AtBu was purchased from CheMatech Inc. (Dijon,

France) for peptide synthesis. ^{125}I-Tyr^2-[Nle^4, D-Phe^7]-α-MSH {^{125}I-(Tyr^2)-NDP-MSH} was obtained from PerkinElmer, Inc. (Waltham, MA) for receptor binding assay. $^{67}GaCl_3$ was purchased from MDS Nordion, Inc. (Vancouver, Canada) for radiolabeling. All other chemicals used in this study were purchased from Thermo Fischer Scientific (Waltham, MA) and used without further purification. B16/F1 murine melanoma cells were obtained from American Type Culture Collection (Manassas, VA).

Peptide Synthesis and Receptor Binding Assay

DOTA-GGNle-CycMSH$_{hex}$ was synthesized, purified by RP-HPLC and characterized by liquid chromatography-mass spectrometry (LC-MS) according to our published procedure.[24] New NOTA-GGNle-CycMSH$_{hex}$ was synthesized using Fmoc chemistry. Briefly, the intermediate scaffold of Fmoc-Asp(O-2-PhiPr)-His(Trt)-DPhe-Arg(Pbf)-Trp(Boc)-Lys(Mtt) was synthesized on H_2N-Novagel resin by an Advanced ChemTech multiple-peptide synthesizer (Louisville, KY). Generally, 70 μmol of resin, 210 μmol of each Fmoc-protected amino acid and NO2AtBu were used for the synthesis. The protecting groups of Mtt and 2-phenylisopropyl were removed by 2.5% of trifluoroacetic acid (TFA) for peptide cyclization. The cyclization reaction was achieved on the resin by an overnight reaction in dimethylformamide (DMF) using benzotriazole-1-yl-oxy-tris-pyrrolidino-phosphonium-hexafluorophosphate (PyBOP) as a coupling agent in the presence of N,N-diisopropylethylamine (DIEA). After the cyclization, the moiety of NO2AtBu-CH_2-Gly-Gly-Nle was coupled to the cyclic intermediate scaffold to yield NO2AtBu-CH_2-Gly-Gly-Nle-Cyclic[Asp-His(Trt)-DPhe-Arg(Pbf)-Trp(Boc)-Lys] on the resin. All protecting groups were totally removed and the peptide was cleaved from the resin by treating with a mixture of trifluoroacetic acid (TFA), thioanisole, phenol, water, ethanedithiol and triisopropylsilane (87.5:2.5:2.5:2.5:2.5:2.5) for 2 h at 25°C. The peptide was precipitated and washed with ice-cold ether four times, purified by RP-HPLC on a Grace Vydac C-18 reverse phase analytical column (Vydac 218TP54: 5 μm, 4.6 mm i.d. × 250 mm), and characterized by LC-MS. The MC1 receptor binding affinity (IC_{50} value) of NOTA-GGNle-CycMSH$_{hex}$was determined in B16/F1 melanoma cells by *in vitro* competitive receptor binding assay according to our published procedure[24] and compared with DOTA-GGNle-CycMSH$_{hex}$.

Effects of Reaction Time and Temperature on ^{67}Ga Radiolabeling Yield

NOTA can form stable complex with ^{67}Ga at lower temperature than DOTA.[28–29] To examine the effects of reaction time and temperature on radiolabeling yield, DOTA-GGNle-CycMSH$_{hex}$and NOTA-GGNle-CycMSH$_{hex}$ were radiolabeled with ^{67}Ga in a 0.5 M NH_4OAc-buffered solution (pH 3.5) at different temperatures for different reaction time points, respectively. Briefly, 10 μL of $^{67}GaCl_3$ (18.5–37.0 MBq in 0.05 M HCl), 10 μL of 1 mg/mL DOTA-GGNle-CycMSH$_{hex}$or NOTA-GGNle-CycMSH$_{hex}$ aqueous solution and 100 μL of 0.5 M NH_4OAc (pH 3.5) were added into a reaction vial and incubated at 25, 37, 45 and 75°C for 5, 15, 30 and 45 min, respectively. After the incubation, 10 μL of 0.5% EDTA aqueous solution was added into each reaction vial to bind unbound $^{67}Ga^{3+}$. The radiolabeling yield of each peptide was determined by Waters RP-HPLC (Milford, MA) on a Grace Vadyc C-18 reverse phase analytical column (Deerfield, IL) using the following gradient at a flow rate of 1 mL/min. The mobile phase consisted of solvent A (20 mM HCl aqueous solution) and solvent B (100% CH_3CN). The gradient was initiated and kept at 82:18 A/B for 3 min followed by a linear gradient of 82:18 A/B to 72:28 A/B over 20 min. Then, the gradient was changed from 72:28 A/B to 10:90 A/B over 3 min followed by an additional 5 min at 10:90 A/B. Thereafter, the gradient was changed from 10:90 A/B to 82:18 A/B over 3 min.

Biodistribution Studies

All animal studies were conducted in compliance with Institutional Animal Care and Use Committee approval. The melanoma targeting and pharmacokinetic properties of ^{67}Ga-DOTA-GGNle-CycMSH$_{hex}$ and ^{67}Ga-NOTA-GGNle-CycMSH$_{hex}$ were determined in B16/F1 melanoma-bearing C57 female mice (Harlan, Indianapolis, IN). The C57 mice were subcutaneously inoculated with 1×10^6 B16/F1 cells on the right flank for each mouse to generate B16/F1 tumors. The weights of tumors reached approximately 0.2 g 10 days post cell inoculation. Each melanoma-bearing mouse was injected with 0.037 MBq of ^{67}Ga-DOTA-GGNle-CycMSH$_{hex}$ or ^{67}Ga-NOTA-GGNle-CycMSH$_{hex}$ via the tail vein. Groups of 5 mice were sacrificed at 0.5, 2, 4 and 24 h post-injection, and tumors and organs of interest were harvested, weighed and counted. Blood values were taken as 6.5% of the whole-body weight. The specificity of tumor uptake of ^{67}Ga-DOTA-GGNle-CycMSH$_{hex}$ or ^{67}Ga-NOTA-GGNle-CycMSH$_{hex}$ was determined by co-injecting 10 μg (6.07 nmol) of unlabeled NDP-MSH peptide at 2 h post-injection.

Melanoma Imaging with ^{67}Ga-NOTA-GGNle-CycMSH$_{hex}$

^{67}Ga-NOTA-GGNle-CycMSH$_{hex}$exhibited more favorable radiolabeling conditions (> 85% radiolabeling yields at 37°C for 30 min), as well as higher tumor/kidney uptake ratio than ^{67}Ga-DOTA-GGNle-CycMSH$_{hex}$ at 2 h post-injection. Thus, we further evaluated the melanoma imaging property of ^{67}Ga-NOTA-GGNle-CycMSH$_{hex}$. Approximately 11.1 MBq of ^{67}Ga-NOTA-GGNle-CycMSH$_{hex}$ was injected into a B16/F1 melanoma-bearing mouse via the tail vein. The mouse was euthanized for small animal SPECT/CT (Nano-SPECT/CT®, Bioscan) imaging at 2 h post-injection. The CT imaging was immediately followed by single photon emission computed tomography (SPECT) imaging of whole-body. The SPECT scans of 24 projections were acquired. Reconstructed SPECT and CT data were visualized and co-registered using InVivoScope (Bioscan, Washington DC).

Statistical Analysis

Statistical analysis was performed using the Student's t-test for unpaired data. A 95% confidence level was chosen to determine the significance of the difference in tumor and renal uptake between ^{67}Ga-NOTA-GGNle-CycMSH$_{hex}$ and ^{67}Ga-DOTA-GGNle-CycMSH$_{hex}$, as well as the significance of the difference in tumor uptake between ^{67}Ga-NOTA-GGNle-CycMSH$_{hex}$ with/without NDP-MSH co-injection, and between ^{67}Ga-DOTA-GGNle-CycMSH$_{hex}$ with/without NDP-MSH co-injection. The differences at the 95% confidence level ($p<0.05$) were considered significant.

RESULTS

New NOTA-GGNle-CycMSH$_{hex}$ was synthesized and purified by RP-HPLC. NOTA-GGNle-CycMSH$_{hex}$ displayed greater than 90% chemical purity after HPLC purification with 30% synthetic yield. The identity of NOTA-GGNle-CycMSH$_{hex}$ was confirmed by electrospray ionization mass spectrometry. The calculated and found molecular weights of NOTA-GGNle-CycMSH$_{hex}$ were 1381 and 1381, respectively. Meanwhile, DOTA-GGNle-CycMSH$_{hex}$ was synthesized and characterized according to our published procedure[24] for comparison. The calculated and found molecular weights of DOTA-GGNle-CycMSH$_{hex}$ were 1368 and 1368, respectively. The schematic structures of NOTA-GGNle-CycMSH$_{hex}$ and DOTA-GGNle-CycMSH$_{hex}$ are shown in Figure 1. The IC_{50} value of NOTA-GGNle-CycMSH$_{hex}$ was 1.6 nM in B16/F1 melanoma cells, which was comparable to that of DOTA-GGNle-CycMSH$_{hex}$ (2.1 nM).[24]

The effects of reaction time and temperature on radiolabeling yields are presented in Figure 2. The radiolabeling yield of ^{67}Ga-DOTA-GGNle-CycMSH$_{hex}$ or ^{67}Ga-NOTA-GGNle-

$CycMSH_{hex}$ was reaction time-dependent at 25°C, 37°C, 45°C and 75°C, respectively. The radiolabeling yield improved when the reaction time prolonged from 5 min to 45 min. For instance, as showed in Figure 2 at 25°C, the radiolabeling yield of ^{67}Ga-NOTA-GGNle-$CycMSH_{hex}$was 27% after 5 min incubation, and was 70% after 45 min incubation. Meanwhile, the time-dependent fashion was observed for ^{67}Ga-DOTA-GGNle-$CycMSH_{hex}$ as well despite the fact that the radiolabeling yield of ^{67}Ga-DOTA-GGNle-$CycMSH_{hex}$ was lower than 5% at 25°C even after 45 min incubation. The radiolabeling yield of ^{67}Ga-DOTA-GGNle-$CycMSH_{hex}$ or ^{67}Ga-NOTA-GGNle-$CycMSH_{hex}$ was reaction temperature-dependent after 5, 15, 30 and 45 min incubation, respectively. The radiolabeling yield increased when the reaction temperature elevated from 25°C to 75°C. For example, as showed in Figure 2 after 30 min incubation, the radiolabeling yield of ^{67}Ga-NOTA-GGNle-$CycMSH_{hex}$was 67% at 25°C and was 91% at 75°C. Similarly, the radiolabeling yield of ^{67}Ga-DOTA-GGNle-$CycMSH_{hex}$was less than 5% at 25°C and was 97% at 75°C. Overall, the radiolabeling yield of ^{67}Ga-NOTA-GGNle-$CycMSH_{hex}$ could reach greater than 85% started from 37°C, whereas the radiolabeling yield of ^{67}Ga-DOTA-GGNle-$CycMSH_{hex}$ could achieve greater than 84% only at 75°C. After we examined the effects of reaction time and temperature on radiolabeling yield, we performed peptide radiolabeling at 75°C for 30 min for biodistribution and imaging studies. DOTA-GGNle-$CycMSH_{hex}$ and NOTA-GGNle-$CycMSH_{hex}$ were readily labeled with ^{67}Ga in a 0.5 M NH_4OAc-buffered solution (pH 3.5) with greater than 90% radiolabeling yields. ^{67}Ga-DOTA-GGNle-$CycMSH_{hex}$ and ^{67}Ga-NOTA-GGNle-$CycMSH_{hex}$ were completely separated from their excess non-labeled peptides by RP-HPLC. The retention times of ^{67}Ga-DOTA-GGNle-$CycMSH_{hex}$ and ^{67}Ga-NOTA-GGNle-$CycMSH_{hex}$ were 16.3 and 16.4 min, respectively.

The melanoma targeting and pharmacokinetic properties of ^{67}Ga-DOTA-GGNle-$CycMSH_{hex}$ and ^{67}Ga-NOTA-GGNle-$CycMSH_{hex}$ were determined in B16/F1 melanoma-bearing C57 mice. The biodistribution results of ^{67}Ga-DOTA-GGNle-$CycMSH_{hex}$ and ^{67}Ga-NOTA-GGNle-$CycMSH_{hexb}$ are presented in Table 1. ^{67}Ga-DOTA-GGNle-$CycMSH_{hex}$ exhibited rapid high melanoma uptake and prolonged tumor retention. The tumor uptake of ^{67}Ga-DOTA-GGNle-$CycMSH_{hex}$ was 26.96 ± 3.82 % ID/g at 0.5 h post-injection. ^{67}Ga-DOTA-GGNle-$CycMSH_{hex}$ displayed similar high tumor uptake (25.53 ± 2.22 and 25.13 ± 4.13 % ID/g) at 2 and 4 h post-injection. Even at 24 h post-injection, there was 7.54 ± 1.19 % ID/g of ^{67}Ga-DOTA-GGNle-$CycMSH_{hex}$ activity remained in the tumor. Approximately 96.3% of the tumor uptake of ^{67}Ga-DOTA-GGNle-$CycMSH_{hex}$ was blocked by 10 μg (6.07 nmol) of non-radiolabeled NDP-MSH ($p<0.05$) (Figure 3), demonstrating that the tumor uptake was specific and MC1 receptor-mediated. Whole-body clearance of ^{67}Ga-DOTA-GGNle-$CycMSH_{hex}$ was rapid, with 84.9% of the injected radioactivity cleared through the urinary system by 2 h post-injection. Normal organ uptake of ^{67}Ga-DOTA-GGNle-$CycMSH_{hex}$ was lower than 1.68 % ID/g except for the kidneys at 2, 4 and 24 h post-injection. The kidney uptake was 8.90 ± 1.81 % ID/g at 2 h post-injection and decreased to 5.60 ± 1.24 % ID/g at 24 h post-injection. High tumor uptake and prolonged retention coupled with rapid whole-body clearance resulted in high tumor/blood and high tumor/normal organ uptake ratios achieved as early as 0.5 h post-injection. The tumor/kidney uptake ratio of ^{67}Ga-DOTA-GGNle-$CycMSH_{hex}$ was 1.64, 2.87, 2.98 and 1.35 at 0.5, 2, 4 and 24 h post-injection, respectively.

^{67}Ga-NOTA-GGNle-$CycMSH_{hex}$ showed comparable high melanoma uptake with ^{67}Ga-DOTA-GGNle-$CycMSH_{hex}$ at 2 and 24 h post-injection. The tumor uptake of ^{67}Ga-NOTA-GGNle-$CycMSH_{hex}$ was 20.59 ± 1.57 % ID/g at 0.5 h post-injection. ^{67}Ga-NOTA-GGNle-$CycMSH_{hex}$ reached its peak tumor uptake of 25.12 ± 1.03 % ID/g at 2 h post-injection. The tumor uptake of ^{67}Ga-NOTA-GGNle-$CycMSH_{hex}$ was 18.17 ± 4.89 and 7.95 ± 2.58 % ID/g at 4 and 24 h post-injection. Approximately 90.8% of the tumor uptake of ^{67}Ga-NOTA-GGNle-$CycMSH_{hex}$ was blocked by 10 μg (6.07 nmol) of non-radiolabeled NDP-MSH

($p<0.05$) (Figure 3), demonstrating that the tumor uptake was specific and MC1 receptor-mediated. Whole-body clearance of ^{67}Ga-NOTA-GGNle-CycMSH$_{hex}$ was rapid, with 84.1% of the injected radioactivity cleared through the urinary system by 2 h post-injection. Normal organ uptakes of ^{67}Ga-NOTA-GGNle-CycMSH$_{hex}$ were lower than 1.62 % ID/g except for the kidneys at 2, 4 and 24 h post-injection. The kidney uptake was 8.34 ± 3.25 % ID/g at 2 h post-injection and decreased to 2.74 ± 0.64 % ID/g at 24 h post-injection. High tumor uptake and prolonged retention coupled with rapid whole-body clearance resulted in high tumor/blood and high tumor/normal organ uptake ratios achieved as early as 0.5 h post-injection. The tumor/kidney uptake ratio of ^{67}Ga-DOTA-GGNle-CycMSH$_{hex}$ was 1.76, 3.01, 2.40 and 2.90 at 0.5, 2, 4 and 24 h post-injection, respectively.

^{67}Ga-NOTA-GGNle-CycMSH$_{hex}$exhibited more favorable radiolabeling conditions (> 85% radiolabeling yields started at 37°C), as well as higher tumor/kidney uptake ratio than ^{67}Ga-DOTA-GGNle-CycMSH$_{hex}$ at 2 h post-injection. Therefore, we further evaluated the melanoma imaging properties of ^{67}Ga-NOTA-GGNle-CycMSH$_{hex}$ at 2 h post-injection. The whole-body, coronal and transversal SPECT/CT images are presented in Figure 5. The melanoma tumors were clearly visualized by SPECT/CT using ^{67}Ga-NOTA-GGNle-CycMSH$_{hex}$ as an imaging probe. ^{67}Ga-NOTA-GGNle-CycMSH$_{hex}$ exhibited high tumor to normal organ uptake ratios except for the kidneys, which was consistent with the biodistribution results.

DISCUSSION

Gallium-67 is an attractive SPECT radionuclide with a half-life of 78.3 h and three gamma-emissions (38% 93 keV, 24% 185 keV and 16% 300 keV) (*30–33*). Meanwhile, ^{67}Ga is also a potential therapeutic radionuclide due to its emissions of Auger and conversion electrons.[27] Both linear and cyclic ^{67}Ga-labeled α-MSH peptides[8,22] have been reported for melanoma imaging over the past several years. Initially, Froidevaux et al. reported the linear ^{67}Ga-DOTA-NAPamide, which exhibited 9.43 ± 1.06 and 3.10 ± 0.36 %ID/g of B16/F1 melanoma uptake at 4 and 24 post-injection, respectively.[8] Thereafter, we reported the lactam bridge-cyclized ^{67}Ga-DOTA-GlyGlu-CycMSH.[22] The B16/F1 melanoma uptake of ^{67}Ga-DOTA-GlyGlu-CycMSH was 14% less than that of ^{67}Ga-DOTA-NAPamide at 4 h post-injection, whereas the B16/F1 melanoma uptake of ^{67}Ga-DOTA-GlyGlu-CycMSH was 1.6 times the melanoma uptake of ^{67}Ga-DOTA-NAPamide at 24 h post-injection. Surprisingly, the renal uptake of ^{67}Ga-DOTA-GlyGlu-CycMSH was 5.7 and 10.3 times the renal uptake of ^{67}Ga-DOTA-NAPamide at 4 and 24 h post-injection, respectively. Dramatic difference in renal uptake between ^{67}Ga-DOTA-GlyGlu-CycMSH and ^{67}Ga-DOTA-NAPamide was likely due to their structural differences.

Recently, we have identified a novel class of lactam bridge-cyclized α-MSH peptides with enhanced melanoma uptake and reduced renal uptake.[23,24] Specifically, ^{111}In-DOTA-GGNle-CycMSH$_{hex}$ exhibited the highest tumor/kidney uptake ratios (2.8 and 2.7 at 2 and 4 h post-injection) among all reported ^{111}In-labeled cyclic peptides.[23,24] Thus, we were interested in determining whether or not ^{67}Ga-DOTA-GGNle-CycMSH$_{hex}$ could display higher melanoma uptake and lower renal uptake compared to ^{67}Ga-DOTA-GlyGlu-CycMSH in this study. Meanwhile, we also evaluated ^{67}Ga-NOTA-GGNle-CycMSH$_{hex}$ because NOTA can also form a stable complex with ^{67}Ga even at lower reaction temperature than DOTA.[28,29] As we anticipated, NOTA-GGNle-CycMSH$_{hex}$ showed comparable MC1 receptor binding affinity with DOTA-GGNle-CycMSH$_{hex}$ (1.6 vs. 2.1 nM). In terms of radiolabeling yield, ^{67}Ga-NOTA-GGNle-CycMSH$_{hex}$ could reach 70% and 85% radiolabeling yields even at 25°C and 37°C, respectively. Meanwhile, the radiolabeling yield of ^{67}Ga-DOTA-GGNle-CycMSH$_{hex}$ could be greater than 85% only at 75°C. At 75°C, both ^{67}Ga-NOTA-GGNle-CycMSH$_{hex}$ and ^{67}Ga-DOTA-GGNle-CycMSH$_{hex}$ could achieve

greater than 90% radiolabeling yield after 30 min incubation. It was important to note that high radiolabeling yield of ^{67}Ga-NOTA-GGNle-CycMSH$_{hex}$at 37°C represented a distinct practical advantage compared to ^{67}Ga-DOTA-GGNle-CycMSH$_{hex}$.

The biodistribution results supported our hypothesis. ^{67}Ga-DOTA-GGNle-CycMSH$_{hex}$ exhibited higher melanoma uptake and lower renal uptake compared to ^{67}Ga-DOTA-GlyGlu-CycMSH. The tumor uptake of ^{67}Ga-DOTA-GGNle-CycMSH$_{hex}$ was 3.1, 2.0 and 3.1 times the tumor uptake of ^{67}Ga-DOTA-GlyGlu-CycMSH at 0.5, 2 and 4 h post-injection, respectively. Meanwhile, the renal uptake of ^{67}Ga-DOTA-GGNle-CycMSH$_{hex}$ was only 69%, 32%, 37% and 27% of the renal uptake of ^{67}Ga-DOTA-GlyGlu-CycMSH at 0.5, 2, 4 and 24 h post-injection, respectively. The increased tumor uptake and decreased renal uptake dramatically improved the tumor to kidney uptake ratios of ^{67}Ga-DOTA-GGNle-CycMSH$_{hex}$ at all time points investigated in this study (Table 1). The tumor to kidney uptake ratio of ^{67}Ga-DOTA-GGNle-CycMSH$_{hex}$ was 4.6, 6.2, 8.3 and 5.6 times those of ^{67}Ga-DOTA-GlyGlu-CycMSH at 0.5, 2, 4 and 24 h post-injection, respectively.

^{67}Ga-NOTA-GGNle-CycMSH$_{hex}$ displayed comparable high melanoma uptake with ^{67}Ga-DOTA-GGNle-CycMSH$_{hex}$ at 2 and 24 h post-injection. Meanwhile, ^{67}Ga-NOTA-GGNle-CycMSH$_{hex}$ exhibited comparable renal uptake with ^{67}Ga-DOTA-GGNle-CycMSH$_{hex}$ at 2 and 4 h post-injection. Interestingly, the renal uptake of with ^{67}Ga-NOTA-GGNle-CycMSH$_{hex}$ was only 71% and 49% of that of ^{67}Ga-DOTA-GGNle-CycMSH$_{hex}$ at 0.5 and 24 h post-injection. The further reduced renal uptake resulted in higher tumor/kidney uptake ratios of ^{67}Ga-NOTA-GGNle-CycMSH$_{hex}$ than ^{67}Ga-DOTA-GGNle-CycMSH$_{hex}$ at 0.5 and 24 h post-injection. Moreover, ^{67}Ga-NOTA-GGNle-CycMSH$_{hex}$ showed slightly higher tumor/kidney uptake ratio than ^{67}Ga-DOTA-GGNle-CycMSH$_{hex}$ at 2 h post-injection (Figure 4). We have demonstrated that *L*-lysine co-injection decreased the renal uptake of ^{67}Ga-DOTA-GlyGlu-CycMSH by 69.8% at 2 h post-injection in our previous report.[22] In this study, the renal uptake of ^{67}Ga-NOTA-GGNle-CycMSH$_{hex}$ and ^{67}Ga-DOTA-GGNle-CycMSH$_{hex}$ was only 30% and 32% of the renal uptake of ^{67}Ga-DOTA-GlyGlu-CycMSH at 2 h post-injection (Figure 4). Dramatic difference in renal uptake among ^{67}Ga-DOTA-GlyGlu-CycMSH, ^{67}Ga-NOTA-GGNle-CycMSH$_{hex}$ and ^{67}Ga-DOTA-GGNle-CycMSH$_{hex}$ was likely due to their structural differences.

Despite the fact that the melanoma lesions could be visualized by SPECT/CT using ^{67}Ga-DOTA-GlyGlu-CycMSH as an imaging probe,[22] ^{67}Ga-NOTA-GGNle-CycMSH$_{hex}$ exhibited higher tumor imaging contrast (Figure 5) than ^{67}Ga-DOTA-GlyGlu-CycMSH. Higher melanoma uptake coupled with lower renal uptake underscored the potential therapeutic application of ^{67}Ga-NOTA-GGNle-CycMSH$_{hex}$. It will be interesting to examine the therapeutic efficacy of ^{67}Ga-NOTA-GGNle-CycMSH$_{hex}$ in melanoma-bearing mouse model taking advantage of the therapeutic properties of ^{67}Ga in the future. Another potential application of NOTA-GGNle-CycMSH$_{hex}$ peptide is to develop ^{68}Ga-NOTA-GGNle-CycMSH$_{hex}$ for positron emission tomography (PET) imaging of melanoma. Gallium-68 is an attractive PET radionuclide with a half-life of 68 min and can be easily obtained via an in-house commercial ^{68}Ge-^{68}Ga generator. The combination of ^{68}Ga-NOTA-GGNle-CycMSH$_{hex}$ with PET, taking advantage of the outstanding imaging properties of PET and receptor-targeting properties of ^{68}Ga-NOTA-GGNle-CycMSH$_{hex}$, will offer an exciting opportunity for sensitive tumor-specific imaging of melanoma metastases.

In conclusion, both ^{67}Ga-NOTA-GGNle-CycMSH$_{hex}$ and ^{67}Ga-DOTA-GGNle-CycMSH$_{hex}$ exhibited dramatically enhanced melanoma uptake and reduced renal uptake than ^{67}Ga-DOTA-GlyGlu-CycMSH in B16/F1 melanoma bearing C57 mice. ^{67}Ga-NOTA-GGNle-CycMSH$_{hex}$exhibited more favorable radiolabeling conditions (> 85% radiolabeling yields

started at 37°C), as well as higher tumor/kidney uptake ratio than ^{67}Ga-DOTA-GGNle-CycMSH$_{hex}$ at 0.5, 2 and 24 h post-injection. High melanoma uptake coupled with low renal uptake highlighted the potential of ^{67}Ga-NOTA-GGNle-CycMSH$_{hex}$for melanoma imaging and therapy.

Acknowledgments

We thank Dr. Jianquan Yang for his technical assistance. This work was supported in part by the NIH grant NM-INBRE P20RR016480/P20GM103451 and University of New Mexico HSC RAC Award. The image in this article was generated by the Keck-UNM Small Animal Imaging Resource established with funding from the W.M. Keck Foundation and the University of New Mexico Cancer Research and Treatment Center (NIH P30 CA118100).

REFERENCES

1. Giblin MF, Wang NN, Hoffman TJ, Jurisson SS, Quinn TP. Design and characterization of α-melanotropin peptide analogs cyclized through rhenium and technetium metal coordination. Proc. Natl. Acad. Sci. U.S.A. 1998; 95:12814–12818. [PubMed: 9788997]
2. Chen J, Cheng Z, Hoffman TJ, Jurisson SS, Quinn TP. Melanoma-targeting properties of ^{99m}technetium-labeled cyclic alpha-melanocyte-stimulating hormone peptide analogues. Cancer Res. 2000; 60:5649–5658. [PubMed: 11059756]
3. Chen J, Cheng Z, Owen NK, Hoffman TJ, Miao Y, Jurisson SS, Quinn TP. Evaluation of an ^{111}In-DOTA-rhenium cyclized alpha-MSH analog: a novel cyclic-peptide analog with improved tumor-targeting properties. J. Nucl. Med. 2001; 42:1847–1855. [PubMed: 11752084]
4. Miao Y, Owen NK, Whitener D, Gallazzi F, Hoffman TJ, Quinn TP. In vivo evaluation of ^{188}Re-labeled alpha-melanocyte stimulating hormone peptide analogs for melanoma therapy. Int. J. Cancer. 2002; 101:480–487. [PubMed: 12216078]
5. Froidevaux S, Calame-Christe M, Tanner H, Sumanovski L, Eberle AN. A novel DOTA-alpha-melanocyte-stimulating hormone analog for metastatic melanoma diagnosis. J. Nucl. Med. 2002; 43:1699–1706. [PubMed: 12468522]
6. Cheng Z, Chen J, Miao Y, Owen NK, Quinn TP, Jurisson SS. Modification of the structure of a metallopeptide: synthesis and biological evaluation of ^{111}In-labeled DOTA-conjugated rhenium-cyclized alpha-MSH analogues. J. Med. Chem. 2002; 45:3048–3056. [PubMed: 12086490]
7. Miao Y, Whitener D, Feng W, Owen NK, Chen J, Quinn TP. Evaluation of the human melanoma targeting properties of radiolabeled alpha-melanocyte stimulating hormone peptide analogues. Bioconjug. Chem. 2003; 14:1177–1184. [PubMed: 14624632]
8. Froidevaux S, Calame-Christe M, Schuhmacher J, Tanner H, Saffrich R, Henze M, Eberle AN. A gallium-labeled DOTA-alpha-melanocyte-stimulating hormone analog for PET imaging of melanoma metastases. J. Nucl. Med. 2004; 45:116–123. [PubMed: 14734683]
9. Miao Y, Owen NK, Fisher DR, Hoffman TJ, Quinn TP. Therapeutic efficacy of a ^{188}Re-labeled alpha-melanocyte-stimulating hormone peptide analog in murine and human melanoma-bearing mouse models. J. Nucl. Med. 2005; 46:121–129. [PubMed: 15632042]
10. Froidevaux S, Calame-Christe M, Tanner H, Eberle AN. Melanoma targeting with DOTA-alpha-melanocyte-stimulating hormone analogs: structural parameters affecting tumor uptake and kidney uptake. J. Nucl. Med. 2005; 46:887–895. [PubMed: 15872364]
11. Miao Y, Hylarides M, Fisher DR, Shelton T, Moore H, Wester DW, Fritzberg AR, Winkelmann CT, Hoffman TJ, Quinn TP. Melanoma therapy via peptide-targeted alpha-radiation. Clin. Cancer Res. 2005; 11:5616–5621. [PubMed: 16061880]
12. McQuade P, Miao Y, Yoo J, Quinn TP, Welch MJ, Lewis JS. Imaging of melanoma using ^{64}Cu- and ^{86}Y-DOTA-ReCCMSH(Arg11), a cyclized peptide analogue of alpha-MSH. J. Med. Chem. 2005; 48:2985–2992. [PubMed: 15828837]
13. Miao Y, Hoffman TJ, Quinn TP. Tumor-targeting properties of ^{90}Y- and ^{177}Lu-labeled α-melanocyte stimulating hormone peptide analogues in a murine melanoma model. Nucl. Med. Biol. 2005; 32:485–493. [PubMed: 15982579]
14. Miao Y, Fisher DR, Quinn TP. Reducing renal uptake of ^{90}Y and ^{177}Lu labeled alpha-melanocyte stimulating hormone peptide analogues. Nucl. Med. Biol. 2006; 33:723–733. [PubMed: 16934691]

15. Wei L, Butcher C, Miao Y, Gallazzi F, Quinn TP, Welch MJ, Lewis JS. Synthesis and biologic evaluation of ^{64}Cu-labeled rhenium-cyclized alpha-MSH peptide analog using a cross-bridged cyclam chelator. J. Nucl. Med. 2007; 48:64–72. [PubMed: 17204700]
16. Cheng Z, Xiong Z, Subbarayan M, Chen X, Gambhir SS. ^{64}Cu-labeled alpha-melanocyte-stimulating hormone analog for MicroPET imaging of melanocortin 1 receptor expression. Bioconjug. Chem. 2007; 18:765–772. [PubMed: 17348700]
17. Miao Y, Benwell K, Quinn TP. ^{99m}Tc- and ^{111}In-labeled alpha-melanocyte-stimulating hormone peptides as imaging probes for primary and pulmonary metastatic melanoma detection. J. Nucl. Med. 2007; 48:73–80. [PubMed: 17204701]
18. Miao Y, Shelton T, Quinn TP. Therapeutic efficacy of a ^{177}Lu-labeled DOTA conjugated alpha-melanocyte-stimulating hormone peptide in a murine melanoma-bearing mouse model. Cancer Biother. Radiopharm. 2007; 22:333–341. [PubMed: 17651039]
19. Miao Y, Gallazzi F, Guo H, Quinn TP. ^{111}In-labeled lactam bridge-cyclized alpha-melanocyte stimulating hormone peptide analogues for melanoma imaging. Bioconjug. Chem. 2008; 19:539–547. [PubMed: 18197608]
20. Guo H, Shenoy N, Gershman BM, Yang J, Sklar LA, Miao Y. Metastatic melanoma imaging with an ^{111}In-labeled lactam bridge-cyclized alpha-melanocyte-stimulating hormone peptide. Nucl. Med. Biol. 2009; 36:267–276. [PubMed: 19324272]
21. Guo H, Yang J, Gallazzi F, Prossnitz ER, Sklar LA, Miao Y. Effect of DOTA position on melanoma targeting and pharmacokinetic properties of ^{111}In-labeled lactam bridge-cyclized α-melanocyte stimulating hormone peptide. Bioconjug. Chem. 2009; 20:2162–2168. [PubMed: 19817405]
22. Guo H, Yang J, Shenoy N, Miao Y. Gallium-67-labeled lactam bridge-cyclized alpha-melanocyte stimulating hormone peptide for primary and metastatic melanoma imaging. Bioconjug. Chem. 2009; 20:2356–2363. [PubMed: 19919057]
23. Guo H, Yang J, Gallazzi F, Miao Y. Reduction of the ring size of radiolabeled lactam bridge-cyclized alpha-MSH peptide resulting in enhanced melanoma uptake. J. Nucl. Med. 2010; 51:418–426. [PubMed: 20150256]
24. Guo H, Yang J, Gallazzi F, Miao Y. Effects of the amino acid linkers on melanoma-targeting and pharmacokinetic properties of Indium-111-labeled lactam bridge-cyclized α-MSH peptides. J. Nucl. Med. 2011; 52:608–616. [PubMed: 21421725]
25. Raposinho PD, Xavier C, Correia JD, Falcao S, Gomes P, Santos I. Melanoma targeting with alpha-melanocyte stimulating hormone analogs labeled with fac-[^{99m}Tc(CO)$_3$]$^+$: effect of cyclization on tumor-seeking properties. J. Biol. Inorg. Chem. 2008; 13:449–459. [PubMed: 18183429]
26. Raposinho PD, Correia JD, Alves S, Botelho MF, Santos AC, Santos I. A ^{99m}Tc(CO)$_3$-labeled pyrazolyl–α-melanocyte-stimulating hormone analog conjugate for melanoma targeting. Nucl. Med. Biol. 2008; 35:91–99. [PubMed: 18158948]
27. Mariani G, Bodei L, Adelstein SJ, Kassis AI. Emerging roles for radiometabolic therapy of tumors based on auger electron emission. J. Nucl. Med. 2000; 41:1519–1521. [PubMed: 10994732]
28. Clarke ET, Martell AE. Stabilities of trivalent metal ion complexes of the tetraacetate derivatives of 12-, 13-, and 14-membered tetraazamacrocycles. Inorg. Chim. Acta. 1991; 190:37–46.
29. Clarke ET, Martell AE. Stabilities of the Fe(III), Ga(III) and In(III) chelators of N,N',N"-triazacyclononanetriacetic acid. Inorg. Chim. Acta. 1991; 181:273–280.
30. Green MA, Welch MJ. Gallium radiopharmaceutical chemistry. Int. J. Rad. Appl. Instrum. B. 1989; 16:435–448. [PubMed: 2681083]
31. Anderson CJ, Welch MJ. Radiometal-labeled agents (non-technetium) for diagnostic imaging. Chem. Rev. 1999; 99:2219–2234. [PubMed: 11749480]
32. Eisenwiener K, Prata MI, Buschmann I, Zhang HW, Santos AC, Wenger S, Reubi JC, Mäecke HR. NODAGATOC, a new chelator-coupled somatostatin analogue labeled with [$^{67/68}$Ga] and [^{111}In] for SPECT, PET, and targeted therapeutic applications of somatostatin receptor (hsst2) expression tumors. Bioconjug. Chem. 2002; 13:530–541. [PubMed: 12009943]

33. Zhernosekov K, Aschoff P, Filosofov D, Jahn M, Jennewein M, Adrian HJ, Bihl H, Rösch F. Visualisation of a somatostatin receptor-expressing tumour with ^{67}Ga-DOTATOC SPECT. Eur. J. Nucl. Med. Mol. Imaging. 2005; 32:1129. [PubMed: 16133389]

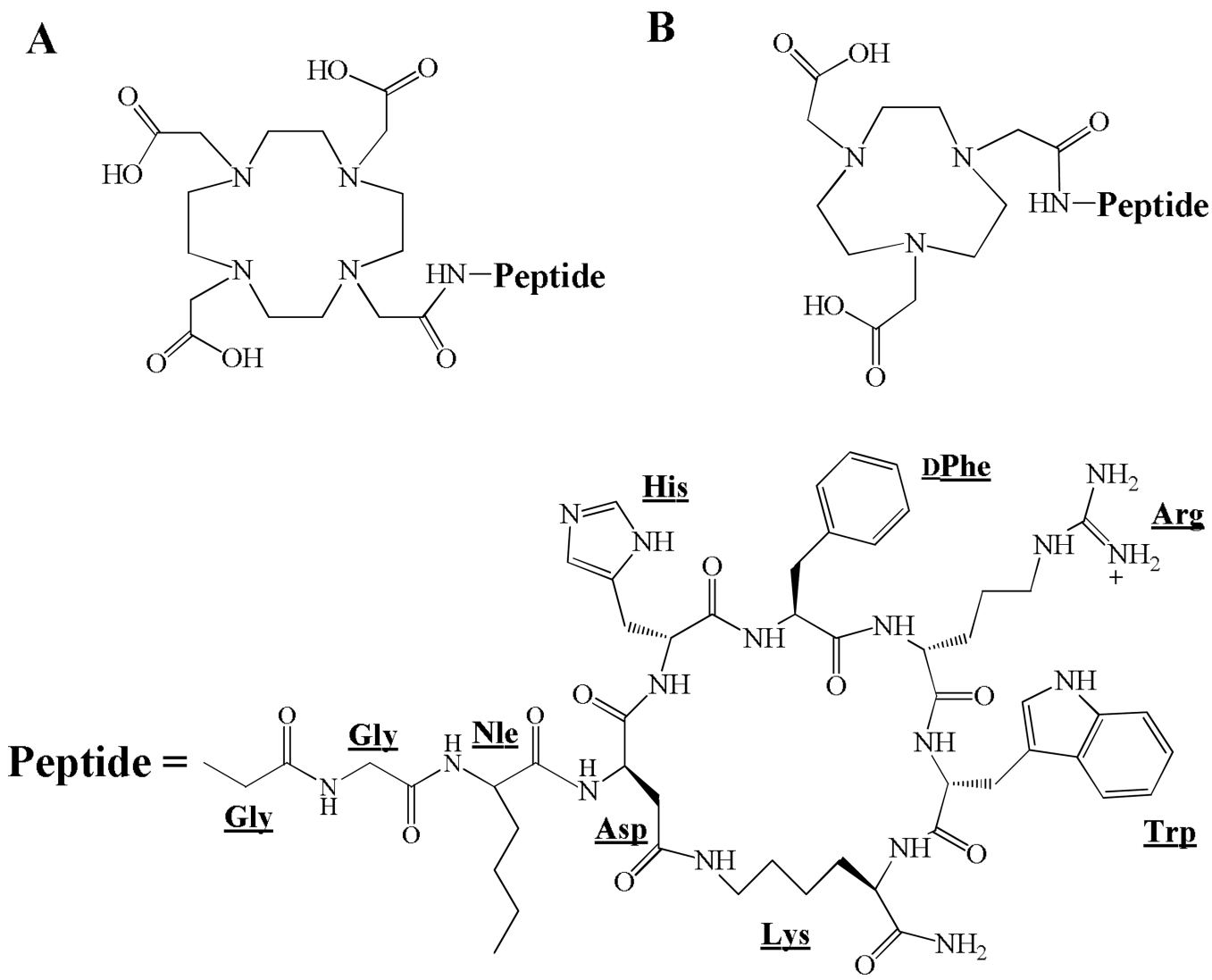

Figure 1.
Schematic structures of DOTA-GGNle-CycMSH$_{hex}$ (A) and NOTA-GGNle-CycMSH$_{hex}$(B).

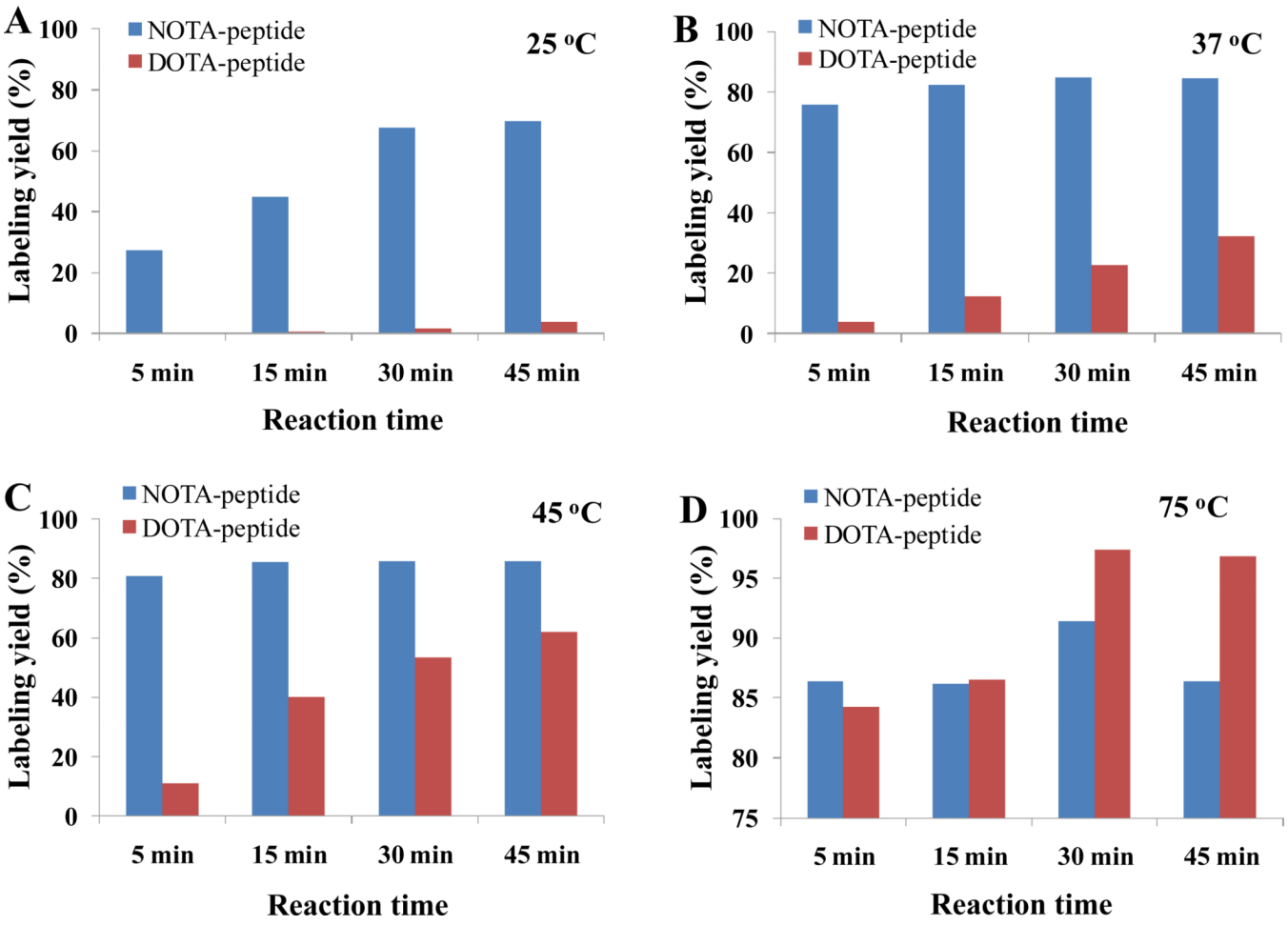

Figure 2.

Effects of reaction time and temperature on radiolabeling yields of ^{67}Ga-DOTA-GGNle-CycMSH$_{hex}$ and ^{67}Ga-NOTA-GGNle-CycMSH$_{hex}$.

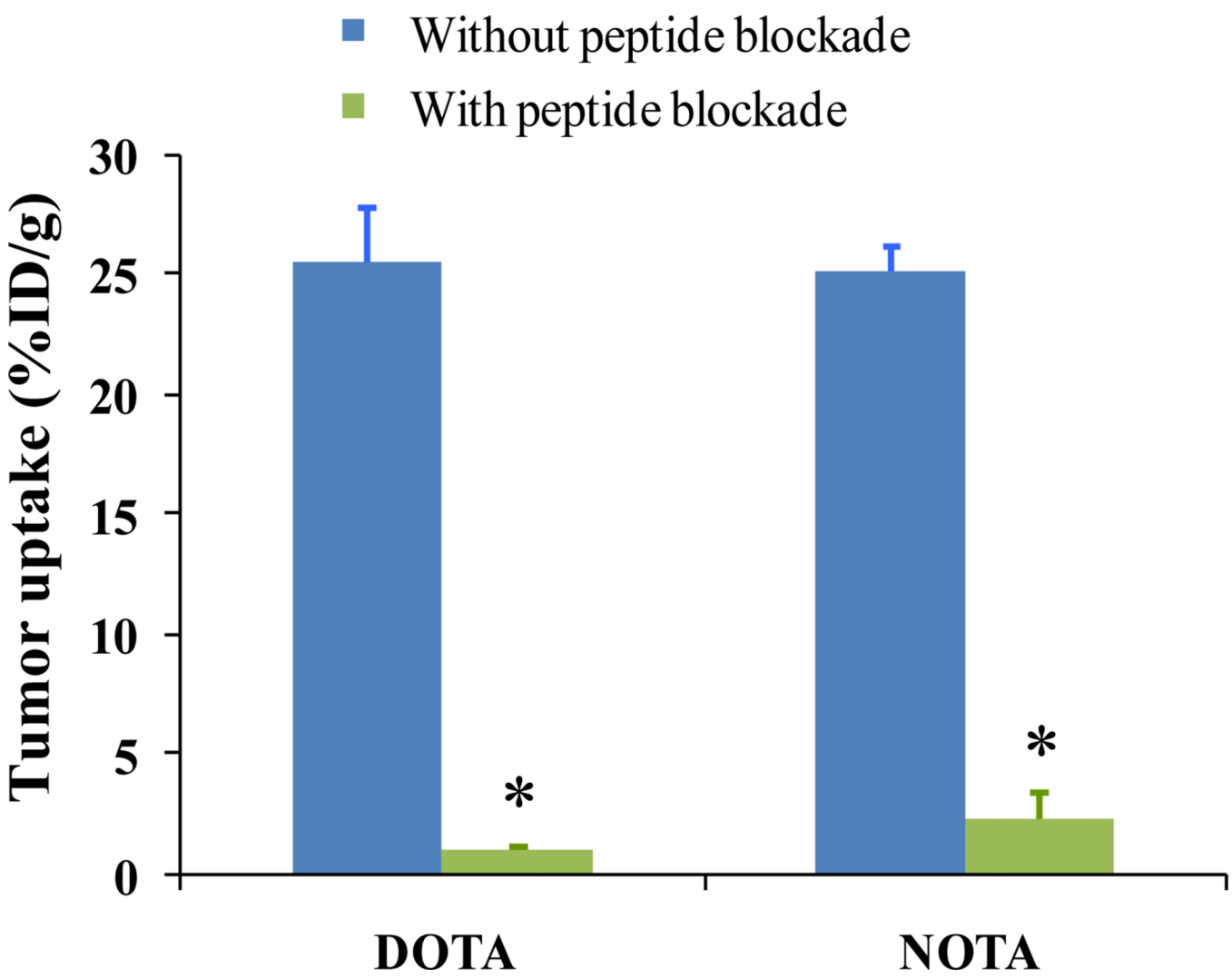

Figure 3.
The tumor uptake of ^{67}Ga-DOTA-GGNle-CycMSH$_{hex}$ (DOTA) and ^{67}Ga-NOTA-GGNle-CycMSH$_{hex}$ (NOTA) with (■) or without (■) 10 μg of NDP-MSH blockade at 2 h post-injection. *p<0.05.

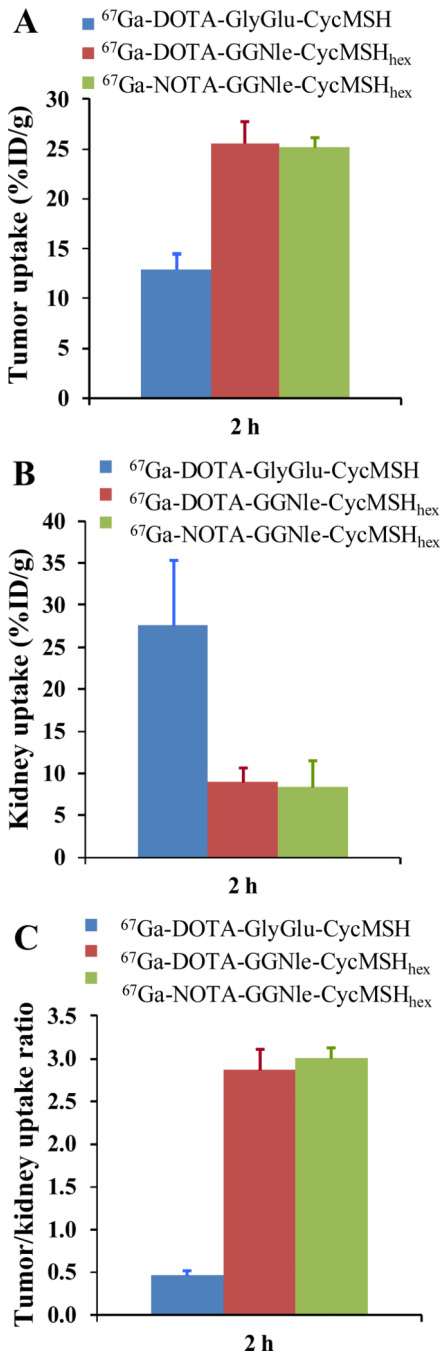

Figure 4.

The comparisons of tumor (A) and kidney (B) uptake, and tumor/kidney uptake ratios (C) at 2 h post-injection among ^{67}Ga-DOTA-GlyGlu-CycMSH (■), ^{67}Ga-DOTA-GGNle-CycMSH$_{hex}$ (■) and ^{67}Ga-NOTA-GGNle-CycMSH$_{hex}$ (■).

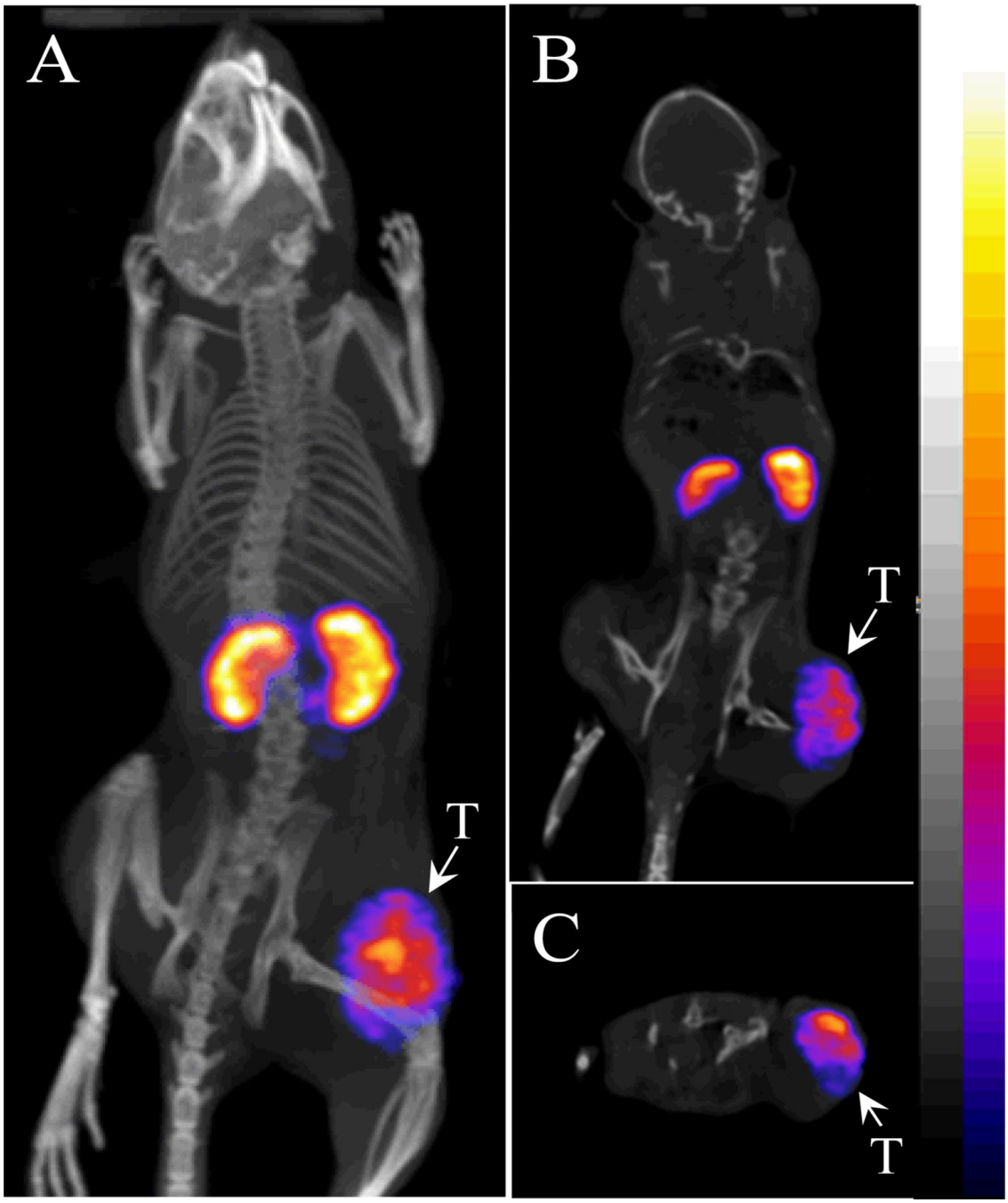

Figure 5.
Representative whole-body (A), coronal (B) and transversal (C) SPECT/CT images of a B16/F1 melanoma-bearing C57 mouse at 2 h post-injection of ^{67}Ga-NOTA-GGNle-CycMSH$_{hex}$. The tumor lesions (T) were highlighted with arrows on the images.

Table 1

Biodistribution of ^{67}Ga-DOTA-GGNle-CycMSH$_{hex}$ and ^{67}Ga-NOTA-GGNle-CycMSH$_{hex}$ in B16/F1 melanoma-bearing C57 mice. The data were presented as percent injected dose/gram or as percent injected dose (Mean ± SD, n=5)

	^{67}Ga-DOTA-GGNle-CycMSH$_{hex}$				**^{67}Ga-NOTA-GGNle-CycMSH$_{hex}$**			
Tissues	**0.5 h**	**2 h**	**4 h**	**24 h**	**0.5 h**	**2 h**	**4 h**	**24 h**
				Percent injected dose/gram (%ID/g)				
Tumor	26.96±3.82	25.53±2.22	25.13±4.13	7.54±1.19	20.59±1.97*	25.12±1.03	18.17±4.89	7.95±2.58
Brain	0.25±0.07	0.15±0.12	0.08±0.03	0.06±0.03	0.21±0.01	0.11±0.07	0.08±0.03	0.08±0.02
Blood	3.33±1.08	0.97±0.91	0.53±0.25	0.29±0.05	2.25±0.09	0.40±0.19	1.02±0.06	0.55±0.12
Heart	1.64±0.18	0.23±0.09	0.24±0.04	0.37±0.08	1.52±0.28	0.45±0.09	0.39±0.17	0.96±0.39
Lung	3.23±0.07	0.40±0.15	0.36±0.08	0.32±0.19	3.71±0.25	0.54±0.04	0.30±0.10	0.35±0.08
Liver	1.82±0.13	0.86±0.19	0.85±0.02	0.54±0.14	1.28±0.14	0.59±0.09	0.54±0.05	0.50±0.12
Spleen	1.39±0.13	0.44±0.09	0.64±0.06	0.52±0.16	1.25±0.11	0.67±0.19	0.57±0.14	0.85±0.23
Stomach	2.51±0.50	1.68±0.50	1.26±0.11	0.62±0.23	1.79±0.22	1.62±0.63	1.45±0.23	1.21±0.40
Kidneys	16.42±2.99	8.90±1.81	8.44±0.11	5.60±1.24	11.67±0.06*	8.34±3.25	7.58±2.70	2.74±0.64*
Muscle	0.75±0.20	0.34±0.10	0.32±0.07	0.30±0.18	0.73±0.26	0.34±0.12	0.33±0.11	0.99±0.56
Pancreas	0.83±0.26	0.34±0.07	0.23±0.06	0.37±0.06	1.03±0.16	0.54±0.13	0.36±0.04	0.88±0.31
Bone	1.44±0.63	1.04±0.24	0.87±0.09	0.72±0.70	1.95±0.08	0.91±0.56	0.96±0.87	0.71±0.24
Skin	5.31±2.35	0.84±0.25	0.81±0.22	0.76±0.21	4.00±0.32	0.54±0.35	0.65±0.24	0.96±0.24
				Percent injected dose (%ID)				
Intestines	1.60±0.30	1.52±1.14	0.98±0.18	0.46±0.06	1.86±0.24	1.22±0.97	0.91±0.05	1.23±0.35
Urine	59.37±5.31	84.91±2.81	87.75±1.44	92.72±1.09	54.16±13.08	84.02±5.71	86.39±3.94	94.57±0.25
				Uptake ratio of tumor/normal tissue				
Tumor/liver	14.84	29.73	29.66	13.86	16.09	42.39	33.40	15.75
Tumor/kidney	1.64	2.87	2.98	1.35	1.76	3.01	2.40	2.90
Tumor/lung	8.35	63.55	69.97	23.35	5.54	46.37	60.24	22.52
Tumor/muscle	35.77	76.04	78.34	25.47	28.19	74.55	54.71	8.05
Tumor/blood	8.10	26.21	47.74	25.56	9.14	62.93	17.75	14.46
Tumor/skin	5.08	30.44	31.10	9.95	5.15	46.35	28.10	8.27

* $P<0.05$ for determining significance of differences in tumor and kidney uptake between ^{67}Ga-DOTA-GGNle-CycMSH$_{hex}$ and ^{67}Ga-NOTA-GGNle-CycMSH$_{hex}$ at the same time point.